Simulation of Protein-Imprinted Polymers. 1. Imprinted Pore Properties

Liora Levi and Simcha Srebnik*

Department of Chemical Engineering, Technion-Israel Institute of Technology, Haifa, Israel 32000

Received: September 10, 2009; Revised Manuscript Received: November 3, 2009

Molecular imprinting is an established method for the creation of artificial recognition sites in synthetic materials through polymerization and cross-linking in the presence of template molecules. Removal of the templates leaves cavities that are complementary to the template molecules in size, shape, and functionality. Although this technique is effective when targeting small molecules, attempts to extend it to larger templates, such as proteins, have failed to show similar success. As opposed to small molecules, proteins are characterized by large size, flexible structure, and large number of functional groups available for recognition, which make it impossible to use imprinting protocols of small molecules for protein imprinting. In this research we use lattice Monte Carlo simulations of an imprinting process using radical polymerization of hydrogels as a simple model for potein-imprinted polymers (PIPs). We investigate the properties of the resulting polymer gel by studying the effects of initiator, cross-linker, and monomer concentrations and the presence of protein on gel structure and porosity. The structure and functionality of the imprinted pore is studied through diffusion of the protein inside the pore immediately following polymerization. The imprinting effect is evaluated by comparing the interaction energy of the protein in the imprinted gel with the energy of a random process.

1. Introduction

The fabrication of molecularly imprinted polymers (MIPs) for the recognition of specific substrates has considerable potential for applications in the areas of clinical analysis, medical diagnostics, environmental monitoring, and drug delivery.[1−7] In particular, molecular imprinting of biomacromolecules and proteins could potentially offer a generic, robust, and cost-effective alternative to existing biological recognition techniques such as monoclonal antibodies.[8−11] The potential application of protein-imprinted polymers (PIPs) as selective protein binding assays is important for isolation, extraction, biosensors, and other laboratory practices, which are almost exclusively dependent on expensive antibodies.[9,10]

Although molecular imprinting of small molecules has advanced significantly over the years and small molecule imprints are currently prepared effectively, efforts to generate imprints of protein targets have been far less successful.[9,11,12] Indeed, studies on protein imprinting show limited success of protein separation and high affinity toward competitor proteins.[11] The encountered difficulties can be attributed to several factors, including the use of water as solvent, which diminishes the power of molecular recognition that mainly relies on electrostatic interactions,[10] the presence of multiple weak interactions on the protein surface, which tends to favor nonspecific binding,[10,11] and the relatively flexible conformation of the macromolecule, which prevents the formation of well-defined recognition sites, compounding the effect of nonspecific recognition. In addition, the large molecular size of the protein results in poor mass transport and permanent entrapment within traditionally dense MIP gels, while high elasticity and porosity of a looser gel makes the imprinting process less selective.[8,10,11] All of these factors contribute to poor performance of the protein-imprinted gel, since optimization with respect to size, shape, and functional group orientation of the template is difficult. Thus, the imprinted cavities show little preferential rebinding to the template protein.

Nonetheless, due to the great potential of PIPs, many research groups have engaged in finding imprinting procedures for proteins,[11] including surface imprinting[13,14] and the epitope[8,10,11] approach. Extensive work on PIPs has focused on polyacrylamide gels due to their biocompetability, neutrality, and inert nature, which apparently minimize nonspecific interactions with proteins.[8,15−20] For example, Ou et al.[17] created acrylate based lysosyme-imprinted polymer by free radical bulk polymerization using charged functional monomers. Selected imprinted polymers gave imprinting factors of 1.83−3.38, exhibiting favorable absorbance of the PIPs in comparison to the nonimprinted polymers (NIPs). However, rebinding was not strictly template specific as the polymer also bound albumin. Furthermore, over 25% of the original template remained in the polymer, contributing further to the poor performance and efficiency of the PIP. Similarly, in competitive adsorption experiments of cytochrome *c* and lysozyme on lysozyme-imprinted polymer, Kimhi and Bianco-Peled[16] showed preferential absorption of the template protein, though, like Ou et al.,[17] it was far less significant compared to cases of imprinting of small molecules, which exhibit selectivity factors close to 20 for enantiomers![21] Takeuchi et al.[19] created an array of imprints, which together were used to determine unique binding profiles for a set of analyte proteins. Though every imprint bound its own template protein with the highest affinity, the selectivity was modest (at most 2.5-fold). By using acidic or basic monomers it was anticipated to find differences in the strength of interactions. However, no clear trend was observed. In another study, Lu et al.[22] used Fe_3O_4 to form PAA gel microspheres with magnetic susceptibility for the imprinting of BSA and lysosyme. Again, while specificity measurements indicated a clear preference of template absorption over the competitor protein, imprinting specificity of the PIPs for both templates was not high, showing an imprinting factor of 2.2.

* To whom correspondence should be addressed. E-mail: simchas@technion.ac.il.

10.1021/jp9087767
Published on Web 11/23/2009

A two-step method[23] for imprinting of proteins (mainly applied to low-content cellular proteins) was recently applied by Long et al.[24] using short vinylic polymeric chains grafted with amino groups for selective assembly with the template protein. Subsequent immobilization of the template−polymer complex into a polymeric microsphere and elution of the template resulted in imprinted polymer gels, which were shown to achieve a high concentration of the target protein in the final solution (>90%). However, no quantitative data on the selectivity or specificity of the PIP were reported, so that imprinting efficiency could not be properly evaluated. As a means to improve the selectivity of weakly cross-linked gels, responsive gels that adsorb small molecular templates upon shrinking when the template is recognized have been developed.[68] It is also important to note that Fu et al.[12] have recently shown that selectivity factor of PIPs when compared with NIPs might appear artificially high if washing procedures used to remove the proteins from the gel are not also used on the nonimprinted polymer.

Molecular simulation offers potential procedures for the rational design of MIPs. Although several computational approaches for MIPs of small molecular templates have been introduced, no simulations of imprinting of macromolecules have been reported to date, while most of the reported computational studies of MIPs rely on fully atomistic models.[25−36] Many of these focus on screening against optimal combinations of functional monomers that will achieve minimal interaction energy of the prepolymerization template−functional monomer complex,[25−31] arguing for a significant correlation between properties of the prepolymerization solution and final imprinting efficiency.[32,37] For example, Li and co-workers[28,29] found that the calculated interaction energy of the template−monomer complex is correlated with the template−polymer binding strength and polymer selectivity, as evaluated by chromatographic experiments. However, Piletsky et al.[30] found that although the calculated monomer−template binding capacity is associated with the retention factor (or binding strength), it has no correlation with the efficiency of MIP specificity. Still, Monti et al.[33] simulated the interaction between a template and building blocks of a prepolymerized complex and showed a qualitative agreement with selective recognition data of their experimental studies.

Recently, Dourado and Sarkisov[38] used a coarse-grained Monte Carlo model that involves formation of MIPs from a prepolymerization solution of functional monomers and cross-linkers in the presence of templates. Adsorption of the templates in the imprinted material showed that molecular recognition occurs between the specific binding sites on the templates and the MIP. An advantage of the simulation model presented in ref 38 is that the distribution of adsorbed molecules among different states of association along the adsorption isotherm can be directly analyzed. A lattice model by Shimizu and co-workers[39] similarly mapped the distribution in site heterogeneity, highlighting the importance of binding site heterogeneity in describing imprinting phenomena. Peppas and co-workers[34,35] used an atomistic kinetic gelation model (KGM) for simulating the free radical polymerization mechanism in a molecular imprinting process of small molecular templates. Their studies revealed specific atomic template−polymer interactions that were then validated by spectroscopic analysis and free energy evaluations of the imprinted network.

In this work, we present a coarse-grained simulation study of PIP formation and characterization using kinetic gelation in coarse-grained lattice Monte Carlo (MC) simulations of free radical polymerization of vinylic molecules (monomers) and divinylic molecules (cross-linkers) in the presence of a globular protein. We present analysis of the extent of gelation and the inner structure of the imprinted gel, evaluated for various preparation conditions. The properties of the imprinted pore, such as pore size and functionality, and interaction energy of the template protein within the imprinted pore are evaluated for different gel compositions and various charge densities of the solution and protein. The protein interaction energy is also compared to theoretical energy values that are calculated for a random particle distribution as a mean to assess the selectivity of the resulting MIP. The selectivity of the imprinted gel with respect to other nontemplate proteins will be addressed in a future communication.

2. Model Description

The assembly of particles to form clusters and networks was traditionally described by lattice bond percolation models in which the polymerization reaction occurs uniformly across the entire system and bonds form randomly between any two adjacent sites.[41] The development of the cluster cluster aggregation (CCA) model[42] based on the original diffusion-limited aggregation model of Witten and Sander[43] offered a different model to simulate aggregation and gelation of particles due to Brownian motion, which resulted in numerous studies considering different particle sticking probabilities, particle functionality, particle diffusivity, and more. These models describe homogeneous polymerization processes, whereby all particles (or bonds) have a similar probability of participating in the gelation. While CCA has been used to study binary systems,[44−46] for the relatively dense PIP systems considered, we found that the CCA model did not result in a cohesive gel and use of kinetic gelation was required.

KGM describes a process of chain growth in which the reaction is restricted to the path of usually a small number of activated particles or sites and in the limit that all particles are activated is identical to the CCA model. Manneville et al.[47] introduced KGM of multifunctional monomers on a simple cubic lattice, where lattice sites represented polymerizing monomers, while no physical movement of monomers was explicitly included. Later models[48−50] integrated vacant lattice sites, thereby allowing for particle movement. Peppas and co-workers[51−53] further modified the original KGM simulation by several means. They included an explicit process of initiation via a first-order decay mechanism of the initiator species and assigned the termination probability for the free radical species.[51,52] Different termination probabilities were tested as a means to account for the differing diffusivities and mobilities of the free radical species, showing only variations in the time dependence of gel formation but not in the final structure.[51] Including initiator decay rate allowed for modeling different free radical reactions, showing for the first time autoacceleration of the reaction at intermediate decay times.[51] Ward et al.[53] extended the KGM model to controlled or "living" free radical polymerization reaction with reversible termination in hopes of producing more homogeneous networks since such methods[54] produce linear polymers with lower polydispersity than conventional free radical polymerization. However, as in their experimental studies,[55] the controlled reaction of a cross-linked network produced heterogeneous networks with similar structural properties to the conventional free radical technique.

One of the first off-lattice simulations to model free radical polymerization was presented by Hutchison and Anseth.[56] Ward and Peppas[38] presented a KGM model and experimental study

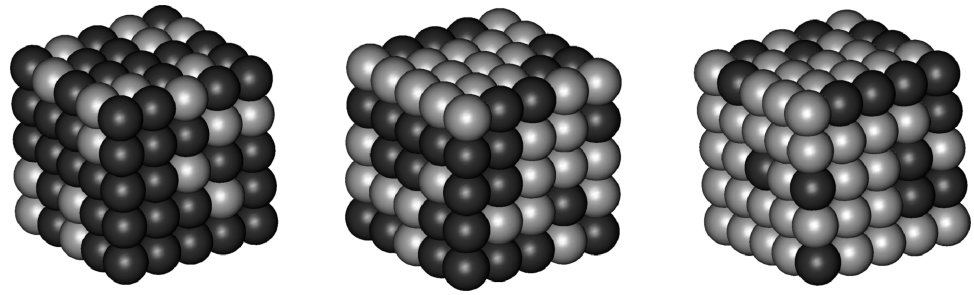

Figure 1. Sample model proteins used in the PIP simulation. Charged residues are represented by light gray spheres and neutral residues by dark gray. From left to right, protein charge density $\rho_p = 0.3$, 0.5, and 0.7.

of polymerization in the presence of a small inert analyte, such as a drug, for controlled release applications in hydrogels. Interestingly, they showed that the presence of the inert solute delayed the gelation point to higher conversions by hindering monomer diffusion. Similarly, the size of the solute delayed gelation but only for lower cross-linking agent concentration. Highly cross-linked networks did not show a substantial delay in the gel point. Recently, Peppas and Henthorn[34,35] adapted the KGM model to atomistic simulations of MIPs.

Our simulation presents a simple lattice model for experimental studies of protein imprinting via acrylate-based bulk radical polymerization.[16,17,20] The occupied lattice sites represent monomers and residues of a globular protein, while empty lattice sites correspond to solvent molecules. The monomers consist of bifunctional monomers and tetrafunctional cross-linkers, simulating free radical copolymerization of vinylic and divinylic monomers, as in previous models.[48−50] The monomers are either neutral or functional (charged), and the cross-linkers are all neutral. The protein is modeled as a globular heteropolymer composed of neutral and charged residues. The shape of the protein is taken to be a rigid cube for simplicity where each residue is represented by a single lattice site (Figure 1). Conformational fluctuations are expected to be negligible due to the confined environment of the protein.[57] The charged protein residues are distributed on the protein shell according to a random distribution and a prescribed charge density. All simulations were performed on a 20^3 lattice, which was found to be sufficient for eliminating the effect of lattice boundaries on gel characteristics.[58]

Initially, the protein and monomers were distributed randomly in the cubic lattice. Prior to gelation, the system was equilibrated, allowing for noncovalent complexation between the template protein and the functional monomers. Equilibration was achieved using 10^5 Monte Carlo (MC) iterations whereby movement of a randomly selected monomer into one of the six neighboring sites is attempted with a Metropolis acceptance criterion under periodic boundary conditions.[59] Moves resulting in particle overlap are always rejected. The only contribution to the energy is nearest neighbor interactions between functional monomers and protein residues. The goal of this stage is to isolate the effect of complex formation. In this simple model, only attractive interactions were considered between functional monomers and protein residues, since noncovalent monomer−monomer interactions and the combination of both attractive and repulsive interactions were found to have a negligible effect on gel structure and pore properties.[58] Accordingly, the energy of a nearest neighbor contact between a functional monomer and a charged protein residue is assigned a value of $-\varepsilon$, while all other nearest neighbor contacts do not contribute to the energy.

Once energetic equilibrium is reached, KGM is used to simulate gelation. The gelation process starts with instantaneous initiation, where radical "signatures" are randomly distributed among the monomers,[47] and continues with propagation, as covalent bonding occurs. Similar to the work of Herman and co-workers,[48] the propagation process integrates two separate steps: particle diffusion, which is conducted according to Metropolis Monte Carlo acceptance rules, and radical bond formation, which takes place upon collision of free radicals with other monomers. The process ends when a single cluster is formed, all free radicals have terminated, or the number of clusters does not change for the next 2×10^5 iterations, which indicates entrapment of all radicals. At this stage of our study, the flexibility of the forming polymer chains is neglected.

The next stage of the simulation involves diffusion of the protein within the imprinted pores in order to calculate the effective pore size and average interaction energy of the protein within the pores.

3. Results and Discussion

For simplicity, only short-ranged interactions are considered. While long-ranged electrostatic forces clearly affect gel properties, leading to the well-known discontinuous volume transition upon change in solvent (or temperature),[60] we consider the properties of the imprinted gel as formed immediately after gelation is complete, in its collapsed state, which provides an indication on the optimal recognition potential.[30,32,37] By using a rigid protein structure we address the aspects of multiple recognition sites, high surface area, and large size of the protein template. The effects of gel and protein flexibility will be addressed in future work.

Gel Properties. The simulated polymerization process integrates particle diffusion and bond formation that takes place upon collision of free radicals with other particles. Referring to the work of Herrmann and co-workers,[48] we define mobility (D) as the ratio of the number of attempted particle moves to the number of bonds grown between attempted moves. We performed several simulations using various values of D in the range of 0−33 in order to analyze the effect of particle mobility on gel structure and on the properties of the imprinted pore. Our findings indicate that gel structure and the extent of gelation are not influenced by the degree of particle mobility and neither is the imprinted pore size and functionality. Accordingly, Herrmann and co-workers[48] found that variations in particle diffusivity have a minor effect on the extent of reaction for any given time of gelation. In view of these results and in order to achieve a rapid gelation process, we considered a polymerization mechanism that executes all allowable propagation steps prior to each attempted move and by which $D \leq 1$ is always achieved. This mechanism corresponds to the case where diffusion is slower than the radical reaction rate, as in diffusion-limited propagation.[61]

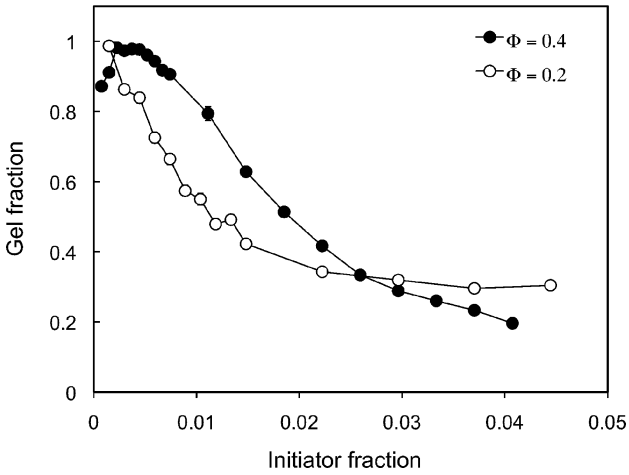

Figure 2. Effect of initiator fraction on final gel fraction, averaged over 200 independent runs.

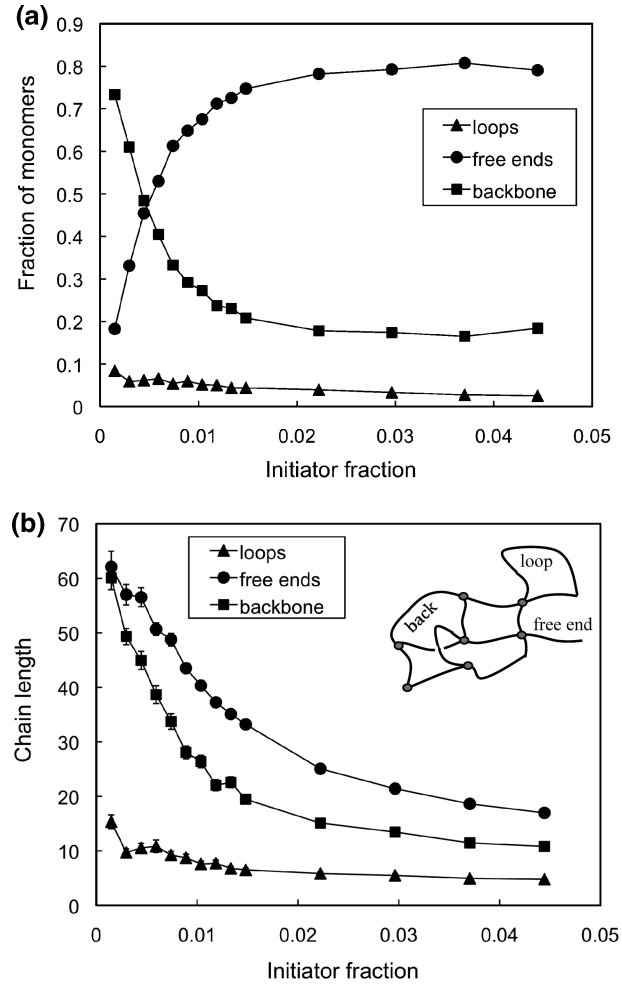

Figure 3. Effect of initiator fraction on the structure of the final gel, averaged over 200 independent runs ($\Phi = 0.2$): (a) average length and (b) composition of backbones, loops, and chain ends (illustrated in inset).

Gelation simulations with various initiator-to-monomer molar ratios indicate that the initiator ratio has a crucial effect on gelation and gel structure (Figures 2 and 3). The gel fraction f_g, or fraction of particles (monomers and cross-linkers) that belong to the main polymerized cluster, provides an estimate for the extent of gelation under various initial conditions. Figure 2 shows the relation between f_g and initiator fraction for two different monomer volume fractions (Φ). We find a significant decrease in f_g at the higher initiator fractions. In fact, for the high particle concentrations considered, maximal initiator concentration corresponding to a CCA-type model results in poor gelation where several separate clusters form. The reduced functionality of the particles (i.e., 2 and 4 instead of 6 on a cubic lattice) along with their restricted mobility within a fairly dense system limit the potential interaction configurations, resulting in poor gelation. Indeed, computational studies based on the CCA model are used to simulate low-density aggregation processes ($\Phi < 0.1$),[44−46] while free radical polymerization mechanisms are often used for simulations of dense systems.[47−50,62−64] Moreover, the optimal initiator molar percent found for our system (Figure 2) agrees with other theoretical studies of gelation by free radical polymerization[48,64,65] as well as with experimental studies of radically polymerized protein-imprinted gels.[16,17]

We can distinguish between three chain types in the cross-linked polymer gel, illustrated in the inset of Figure 3b. The gel backbone is made up of linear chains between two cross-linkers, loop configurations are linear chains that begin and end at the same cross-linker, and free ends are linear chains connected to the gel through only one end. As seen in Figure 3, at low initiator concentrations the fraction of monomers that is part of the final gel is very high and the gel is mainly composed of long backbone chains. Such low initiator concentrations facilitate the formation of a single polymerized unit. Higher initiator concentration leads to a drastic decrease in the length and fraction of monomers that belong to backbone chains, while the fraction of free ends increases substantially. Such chain formations reduce the probability to form a cohesive network, resulting in lower gel fractions. As seen in Figure 3b, the average chain length of all types is significantly reduced when the initiator fraction is increased. That high initiator concentrations shorten the average backbone chain was also indicated by Burdick et al.[66] in an experimental study on chain length distribution formed during the photoinitiated polymerization of divinyl monomers.

According to an early work of KGM simulations by Peppas and co-workers,[51] increasing initiator concentration leads to faster gelation (i.e., higher conversion with time) and reduces kinetic chain length (or length of backbone chains). However, for a given conversion, gel structure was predicted to be the same. For comparison, we calculated the fraction and length of backbone chains, loops, and free ends at a given conversion for various initiator fractions in our model (results not shown). For a given initiator fraction, we surprisingly found that the length of the various types of chains did not change with conversion; however, the number of backbone chains linearly increased while free ends linearly decreased with conversions. Similarly, for a given conversion, we found that increasing the initiator concentration did lead to a decrease in the chain length of all loop types.

Molecular imprinting of small molecules is commonly carried out using a cross-linker percent of up to 95%, resulting in a rigid gel that favors molecule-specific recognition.[67] Such highly cross-linked gels cannot be used for *macro*molecular imprinting due to the limited diffusivity of the large molecules within the gel. For comparison, the commonly used cross-linking percent in protein imprinting methods is only around 5%.[16−18,20] Such low concentrations of cross-linker result in a resilient gel with flexible backbone chains and high swelling ratio. While the high flexibility of the resulting gel enables efficient diffusion of the macromolecules, it also results in impaired specificity and recognition of the template.[8,10,11]

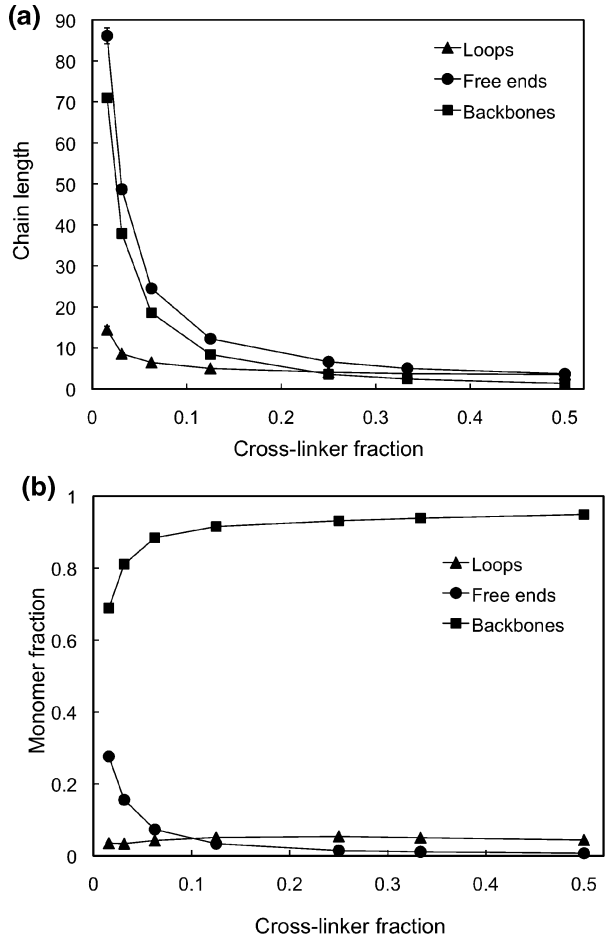

Figure 4. Effect of cross-linker fraction on gel properties, averaged over 200 independent runs ($\Phi = 0.4$): (a) average chain length and (b) composition of the final gel.

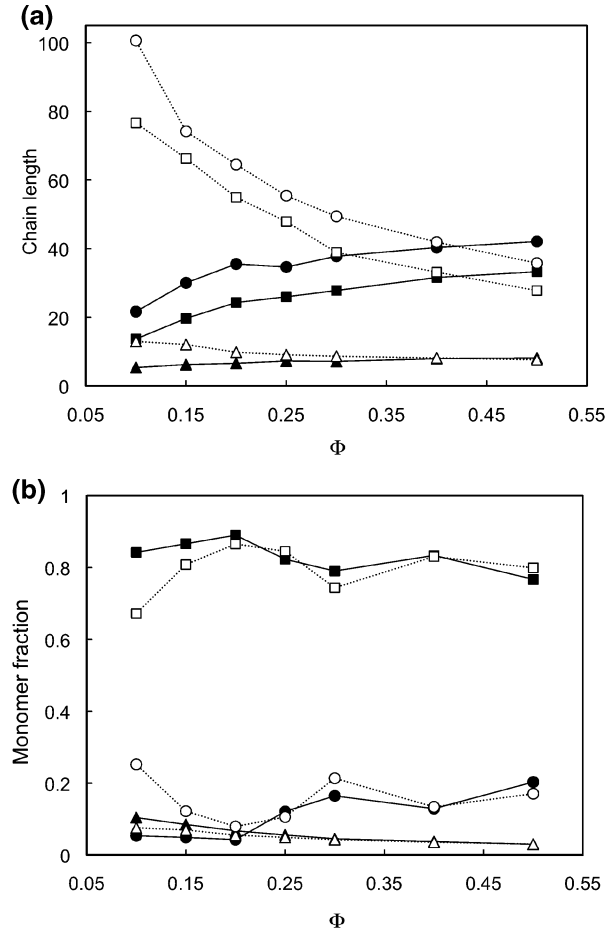

Figure 5. Effect of monomer fraction on gel composition, averaged over 200 independent runs. Gel composition is evaluated through backbone chains (squares), free ends (circles), and loops (triangles) for (a) average chain length and (b) fraction of chain type. Solid and open symbols correspond to a fixed number (200) and fraction (0.15) of cross-linkers, respectively.

Concentrating on low cross-linker concentrations, the effect of cross-linker fraction on gel properties was studied for a constant value of Φ using the optimal initiator fractions for achieving maximal gel fraction. Figure 4a illustrates the effect of increasing fractions of the cross-linking agent on the average chain length within the final gel, showing a rapid decrease in backbone chain length and fraction, due to the increase in the number of cross-links in the forming polymeric chain. This trend, which was also reported in previous experimental studies,[69] suggests that gel flexibility is highly sensitive to the amount of cross-linker. A fairly negligible effect is observed in gel composition (Figure 4b) with the backbone chains remaining the main component. Nonetheless, below 10% cross-linkers the fraction of backbones slightly diminishes in favor of increased free ends due to the reduced probability of cross-linking. Still, even with as low as 1.5% cross-linkers, the backbone chain is significantly dominant, and at 5% cross-linkers the change in the fraction of chain type is ca. 10% from its asymptotic value.

Similarly, the effect of Φ on gel properties was investigated. Figure 5 shows the variation of gel structure with Φ for a fixed number (or concentration) of cross-linkers or a fixed fraction of cross-linkers within the gel. Increasing the monomer volume fraction with a fixed concentration of cross-linkers leads to an increase in the backbone chain length (Figure 5a, solid symbols) due to an increase in the average number of monomers relative to cross-linkers. On the other hand, increasing Φ with a fixed cross-linker fraction leads to a decrease in the chain length (Figure 5a, open symbols) since the cross-linker concentration in this case increases with Φ and hence the probability of forming cross-links increases. However, the composition of the gel remains approximately constant with respect to changes in Φ (Figure 5b). The fact that both cross-linker concentration and Φ have minor effects on the composition of the gel (Figures 4b and 5b) implies that the main influential factor on gel composition is the initiator molar percent (Figure 3a). Accordingly, we find that f_g, which is highly affected by the initiator fraction (Figure 2) and strongly correlated to chain composition (Figure 3a), is hardly influenced by cross-linker fraction or polymer volume fraction.

Simulations were also performed for different functional (divalent) monomer concentrations and indicate that the average gel structure, characterized by chain composition and chain length, is not affected by the concentration of functional monomers. The presence of the protein in the solution during polymerization was found to have no effect on gel structure as well. However, Ward and Peppas[40] carried out KGM simulations combined with experimental studies on the effect of a small inert solute on free radical gelation. Their results indicate that the concentration and size of the solute affects the final structure of the gel by limiting the diffusion rate of monomers and polymer chains during polymerization. They considered the effect of solute at two amounts of cross-linking agents, 10% and 33%. The study revealed that with the higher percentage of cross-linking agent (33%) the solute has little effect on gel structure. In our simulations we consider a dilute protein

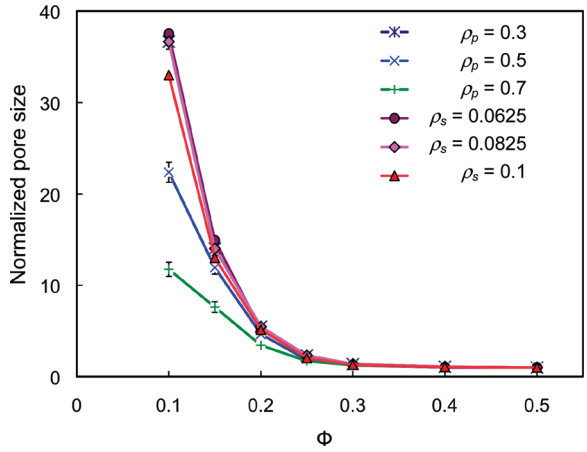

Figure 6. Effect of monomer fraction on imprinted pore size for different fractions of protein charge and solution charge.

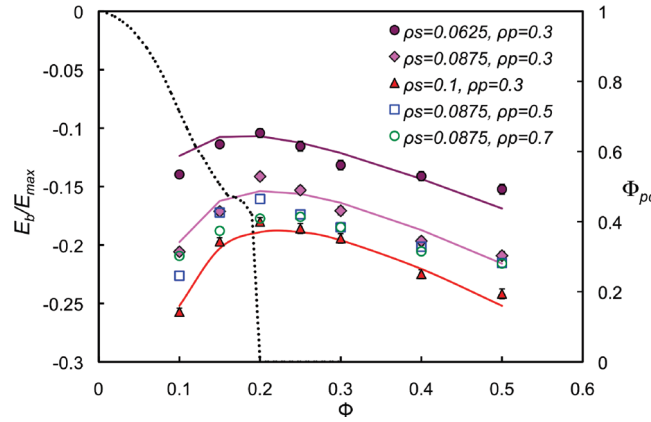

Figure 7. Effect of monomer fraction on protein binding energy within the imprinted pore for various values of protein charge and solution charge. Solid lines correspond to model predictions with $\alpha = 2.4$, 2.1, and 2.1 and $\Phi_{max} = 0.5$. Dashed line shows the fraction of protein-sized percolating pores.

concentration, where the solute (protein) makes up less than 2% of the lattice. While the solute most likely has a local effect on the diffusion rate of monomers and polymer chains, our results indicate that it has a negligible influence on the average structure of the resulting gel at this low concentration. It should be further noted that most of our simulations were carried out for 20% or 40% cross-linker, which according to Figure 4 is beyond the point at which gel structure varied substantially with the amount of cross-linker. Nonetheless, exact comparison with their work is difficult since we studied a considerably less concentrated system (with up to 50% site occupancy compared with 85% of ref 40).

Imprinted Pore Properties. PIP gels were simulated using the KGM protocol in the presence of a rigid model protein (depicted in Figure 1). Diffusion of the template protein within the imprinted pore following polymerization was carried out in order to characterize properties such as effective pore size and association of the imprinted pore with the protein. Note that in the present study of the collapsed form of the gel before swelling the cross-linker fraction does not influence these properties, since the cross-linker concentration does not affect f_g nor the fraction of backbone chains (Figure 4b) but only affects the length of the backbone chains in the gel (Figure 4a). This latter effect will be considered in a future study where gel flexibility and swelling will be simulated.

On the other hand, the polymer volume fraction (Φ) has a significant effect on pore size and functionality, even for a gel in the collapsed state. Unlike the cross-linker fraction, Φ determines the particle density around the protein. Figure 6 shows the average pore size as a function of Φ for various dimensionless charge densities on the protein surface (ρ_p) and in solution (ρ_s). The curves indicate that the imprinted pore size rapidly decreases with increasing polymer density until it reaches a minimum value equal to protein size. Additionally, as seen in Figure 6, a highly charged protein leads to the formation of somewhat smaller pores at low Φ due to increased attraction that brings functional monomers closer to the protein during complexation and polymerization. At high values of Φ, the imprinted pore is tightly wrapped around the template protein.

Figure 7 illustrates the effect of Φ on the binding energy E_b of the protein within the imprinted pore (normalized by protein charge, E_{max}) for different ρ_p and ρ_s. E_b shows a maximum with Φ around 0.2 for the various values of ρ_p and ρ_s. This value of Φ corresponds to a percolation transition (dotted curve in Figure 7) above which there is no percolation of pores that are equal to or larger than protein size. The maximum around the percolation transition observed in Figure 7 can be explained by the following argument. For a fixed concentration of charged monomers, increasing Φ leads to the formation of smaller pores that wrap more tightly around the protein and hence the initial increase in E_b. For $\Phi > 0.2$ the imprinted pores wrap tightly around the protein. A further increase in Φ reduces the charge density of the gel pores since the additional neutral monomers compete for space with the functional monomers. This effect is shown schematically in Figure 8. That is, while high monomer concentrations lead to the formation of smaller pores, the effective functionality of these pores is reduced.

This nonmonotonic dependence of the protein binding energy on Φ can be simply estimated from the two opposing contributions to E_b, i.e., charge density of the gel and imprinted pore size. As argued above, increasing Φ at constant concentration of functional monomers ρ_s leads to a decrease in the effective charge density of the pore, resulting in diminished protein binding probability. That is, in the limit that $\Phi = \rho_s$ the entire gel is functional and the binding energy will roughly depend on the probability of interaction of a monomer with a charged residue. At the other extreme, as Φ approaches unity the gel functionality is negligible for small ρ_s. For a random process, these two limits are obtained with the following relation

$$E_b^* \propto \rho_s E_{max}/(\Phi/\rho_s) \quad (1)$$

where E_b^* is the binding energy for randomly distributed charges and E_{max} is the number of charged residues on the protein surface (or maximal binding capacity of the protein). That is the probability of interaction is reduced by the presence of neutral monomers in solution by a factor of ρ_s/Φ. On the other hand, increasing Φ leads to smaller pores and thus better wrapping around the protein or

$$E_b^* \propto \rho_s E_{max}(\Phi/\Phi_{max}) \quad (2)$$

where Φ_{max} is the monomer concentration for which maximal wrapping of the protein is achieved and depends on the size of the protein. Combining the two terms we obtain

$$\frac{E_b^*}{E_{max}} = -\left(\frac{\rho_s}{\Phi} + \frac{\Phi}{\Phi_{max}}\right)\rho_s \quad (3)$$

Equation 3 provides energetic values for randomly distributed monomers in solution. The effect of equilibration prior to gelation on the binding energy of the imprinted pore may be

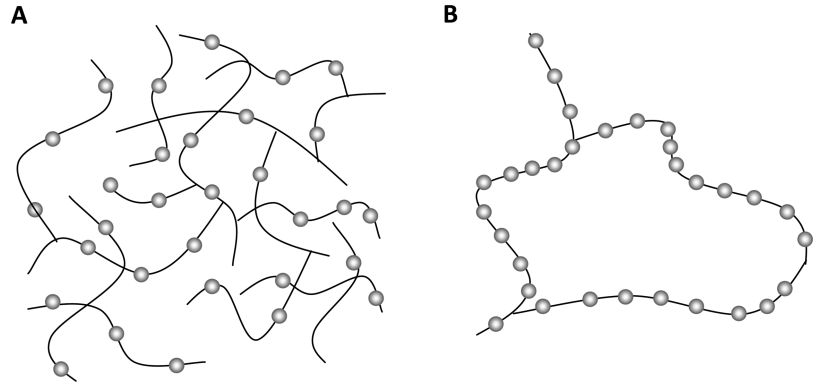

Figure 8. Schematic depiction of a polymer gel prepared with a constant concentration of charged monomers for (a) low Φ and (b) high Φ.

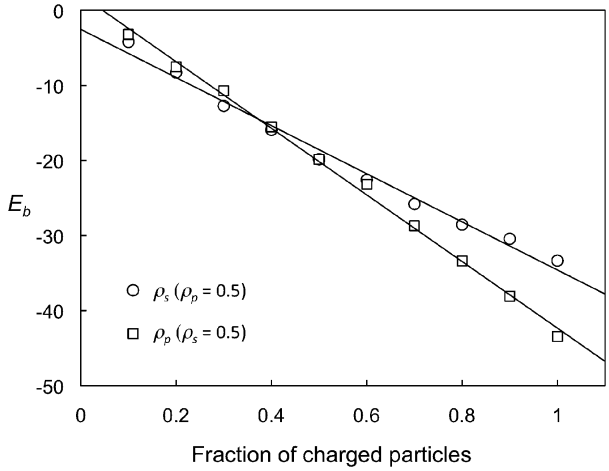

Figure 9. Effect of solution charge (for constant protein charge, circles) and protein charge (for constant solution charge, squares) on protein binding energy within the imprinted pore.

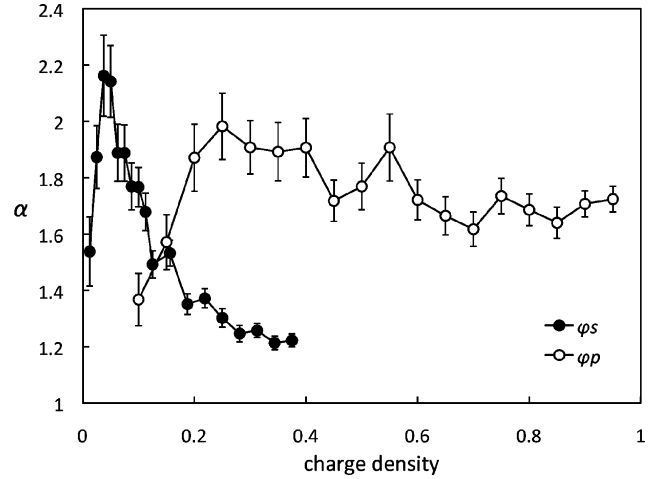

Figure 10. Effect of solution charge and protein charge density on equilibrium factor α. Φ = 0.4.

expressed by $E_b = \alpha E_b^*$, where α is an equilibrium correction factor. Equilibration between the monomers and the template, which is absent in the NIP, is believed to reduce the frustration in the imprinted gel during template adsorption, resulting in lower free energy.[68,70] That is, in the randomly distributed functional groups of the NIP, adsorption of the template would lead to unfavorable interactions between oppositely charged groups of the template and gel. Such interactions are minimized in the imprinted gel.

The solid curves in Figure 7 show the theoretical results fitted to the simulation curves, achieving a good fit with a maximal energetic value around Φ = 0.2 for α ≈ 2. The fact that α > 1 for all Φ values indicates that the equilibrium stage stabilizes the protein−monomer complex and increases the binding capacity of the protein to the resulting imprinted pore. Noting that E_{max} is directly proportional to the protein charge density ρ_p, eq 2 suggests that for constant Φ and small ρ_s the energy of the bound protein is expected to depend linearly on both the fraction of charged monomers in solution and the fraction of charged residues on the protein surface. The expected linear decrease of E_b with the number of charges is seen in Figure 9.

While highly charged solutions and proteins increase the potential number of protein−gel interactions and by that energetically stabilize the protein within the imprinted pore, a highly charged system also increases the amount of nonspecific adsorption. Therefore, the observed decrease in energy in Figure 9 does not necessarily indicate increased imprinting efficiency, which is determined by the ratio of specific to nonspecific absorption.

During the equilibrium stage, a monomer−protein complex is formed and the system transforms from a random configuration to one that is complementary to the protein template. By pointing out the difference between the random configuration and the equilibrated one, the equilibrium factor, α, provides an indication of the impact of the imprinting process. We can approximate the value of α from simulation results of binding energy according to $\alpha = E_b/E_b^*$, where E_b^* is the simulated binding energy of the protein within randomly distributed monomers (corresponding to statistical configuration of functional monomers in solution prior to equilibration and gelation) and E_b is the binding energy in PIP. The results for various charge densities on the protein surface and in solution are shown in Figure 10, exhibiting α > 1 for the entire range studied, as expected. Nonetheless, we see that at low charge densities the probability to form nonspecific interactions is small and the effect of equilibration prior to gelation is negligible (α ≈ 1), and hence, we observe an initial increase in α with charge due to the increase of specific binding. For $\rho_p > 0.25$, α slightly decreases, implying that for a sufficiently charged system protein charge has a relatively minor influence on the equilibrium process. On the other hand, α reaches a sharp peak with ρ_s, indicating that the effect of equilibrium is strong in weakly charged solutions. Thus, we may anticipate that increasing solution charge will diminish the advantage of imprinted polymers over nonimprinted ones. A similar conclusion for protein imprinting was also reported by Kofinas and co-workers,[20] which showed that increasing the charge density of the imprinted gel reduces recognition and impairs imprinting selectivity. Furthermore, this effect is similar to the nonmonotonic behavior observed with polymers imprinted, e.g., with L-phenylalanine anilide using methacrylic acid (MAA) as the functional monomer.[71]

The initial increase in MAA leads to improved selectivity of the polymer toward the template. However, MAA in excess of 20−30% leads to a decrease in selectivity due to the increasing number of nonspecific functional sites.

4. Conclusions

We developed a simple MC-KGM simulation for molecular imprinting of proteins. In the present study, we focused on the structure and functionality of the imprinted pore immediately following complexation and polymerization. The interaction of the protein with the imprinted pore was shown to be influenced by polymer density, with minimal recognition achieved below the protein-sized pore percolation limit of the gel. Additionally, we found that the protein−pore binding energy linearly decreases when increasing charge densities in the solution and on the protein. We defined an equilibrium factor α which measures the extent of recognition in imprinted gels compared to randomly distributed monomers. Solution charge concentration was shown to have a significant influence on α, achieving a maximum value at relatively low charge densities. This result indicates that highly charged solutions will result in increased nonspecific interactions and reveals the advantage of low charged gels over highly charged ones for imprinting of proteins, as experimentally observed. While our current model did not explore the selectivity of the imprinted pore with respect to nontemplate proteins, our model suggests that imprinting based on the multiplicity of nonspecific functional monomers is not sufficient to achieve high imprinting factors. Rather, it appears necessary to find other strategies and protocols that will differentiate between proteins.

References and Notes

(1) Alexander, C.; Andersson, H. S.; Andersson, L. I.; Ansell, R. J.; Kirsch, N.; Nicholls, I. A.; O'Mahony, J.; Whitcombe, M. J. *J. Mol. Recognit.* **2006**, *19* (2), 106.

(2) Jiang, X. M.; Jiang, N.; Zhang, H. X.; Liu, M. C. *Anal. Bioanal. Chem.* **2007**, *389* (2), 355.

(3) Hilt, J. Z.; Byrne, M. E. *Adv. Drug Delivery Rev.* **2004**, *56* (11), 1599.

(4) Alvarez-Lorenzo, C.; Concheiro, A. *J. Chromatogr. B: Anal. Technol. Biomed. Life Sci.* **2004**, *804* (1), 231.

(5) Sellergren, B.; Allender, C. J. *Adv. Drug Delivery Rev.* **2005**, *57* (12), 1733.

(6) Duarte, A. R. C.; Casimiro, T.; Aguiar-Ricardo, A.; Simplicio, A. L.; Duarte, C. M. M. *J. Supercrit. Fluids* **2006**, *39* (1), 102.

(7) Zhang, H. Q.; Ye, L.; Mosbach, K. *J. Mol. Recognit.* **2006**, *19* (4), 248.

(8) Bossi, A.; Bonini, F.; Turner, A. P. F.; Piletsky, S. A. *Biosens. Bioelectron.* **2007**, *22* (6), 1131.

(9) Hansen, D. E. *Biomaterials* **2007**, *28* (29), 4178.

(10) Turner, N. W.; Jeans, C. W.; Brain, K. R.; Allender, C. J.; Hlady, V.; Britt, D. W. *Biotechnol. Prog.* **2006**, *22* (6), 1474.

(11) Zhou, X.; Li, W. Y.; He, X. W.; Chen, L. X.; Zhang, Y. K. *Sep. Purif. Rev.* **2007**, *36* (3−4), 257.

(12) Fu, G. Q.; Yu, H.; Zhu, J. *Biomaterials* **2008**, *29* (13), 2138.

(13) Hirayama, K.; Burow, M.; Morikawa, Y.; Minoura, N. *Chem. Lett.* **1998**, (8), 731.

(14) Shi, H. Q.; Tsai, W. B.; Garrison, M. D.; Ferrari, S.; Ratner, B. D. *Nature* **1999**, *398* (6728), 593.

(15) Janiak, D. S.; Kofinas, P. *Anal. Bioanal. Chem.* **2007**, *389* (2), 399.

(16) Kimhi, O.; Bianco-Peled, H. *Langmuir* **2007**, *23* (11), 6329.

(17) Ou, S. H.; Wu, M. C.; Chou, T. C.; Liu, C. C. *Anal. Chim. Acta* **2004**, *504* (1), 163.

(18) Pang, X. S.; Cheng, G. X.; Lu, S. L.; Tang, E. J. *Anal. Bioanal. Chem.* **2006**, *384* (1), 225.

(19) Takeuchi, T.; Goto, D.; Shinmori, H. *Analyst* **2007**, *132* (2), 101.

(20) Janiak, D. S. Ayyub, O. B. Kofinas, P. Submitted for publication.

(21) Maier, N. M.; Lindner, W. *Anal. Bioanal. Chem.* **2007**, *389* (2), 377.

(22) Lu, S. L.; Cheng, G. X.; Pang, X. S. *J. Appl. Polym. Sci.* **2006**, *99* (5), 2401.

(23) Haupt, K. *Nat. Biotechnol.* **2002**, *20* (9), 884.

(24) Long, Y.; Xing, X. C.; Han, R. F.; Sun, Y.; Wang, Y.; Zhao, Z.; Mi, H. F. *Anal. Biochem.* **2008**, *380* (2), 268.

(25) Wei, S. T.; Jakusch, M.; Mizaikoff, B. *Anal. Chim. Acta* **2006**, *578* (1), 50.

(26) Chianella, I.; Lotierzo, M.; Piletsky, S. A.; Tothill, I. E.; Chen, B. N.; Karim, K.; Turner, A. P. F. *Anal. Chem.* **2002**, *74* (6), 1288.

(27) Pavel, D.; Lagowski, J. *Polymer* **2005**, *46* (18), 7528.

(28) Wu, L. Q.; Li, Y. Z. *J. Mol. Recognit.* **2004**, *17* (6), 567.

(29) Wu, L. Q.; Sun, B. W.; Li, Y. Z.; Chang, W. B. *Analyst* **2003**, *128* (7), 944.

(30) Piletsky, S. A.; Karim, K.; Piletska, E. V.; Day, C. J.; Freebairn, K. W.; Legge, C.; Turner, A. P. F. *Analyst* **2001**, *126* (10), 1826.

(31) Takeuchi, T.; Dobashi, A.; Kimura, K. *Anal. Chem.* **2000**, *72* (11), 2418.

(32) Molinelli, A.; O'Mahony, J.; Nolan, K.; Smyth, M. R.; Jakusch, M.; Mizaikoff, B. *Anal. Chem.* **2005**, *77* (16), 5196.

(33) Monti, S.; Cappelli, C.; Bronco, S.; Giusti, P.; Ciardelli, G. *Biosens. Bioelectron.* **2006**, *22* (1), 153.

(34) Henthorn, D. B.; Peppas, N. A. *Ind. Eng. Chem. Res.* **2007**, *46* (19), 6084.

(35) Henthorn, D. B. Peppas, N. A. In *Molecularly Imprinted Materials*; Kofinas, P., Sellergren, B., Roberts, M. J., Eds.; Materials Research Society: Pittsburgh, PA, 2004; Vol. 787, p 7.

(36) Herdes, C.; Sarkisov, L. *Langmuir* **2009**, *25* (9), 5352.

(37) Idziak, L.; Benrebouh, A.; Deschamps, F. *Anal. Chim. Acta* **2001**, *435* (1), 137.

(38) Dourado, E. M. A.; Sarkisov, L. *J. Chem. Phys.* **2009**, *130* (21), 214701.

(39) Wu, X. Y.; Carroll, W. R.; Shimizu, K. D. *Chem. Mater.* **2008**, *20* (13), 4335.

(40) Ward, J. H.; Peppas, N. A. *J. Controlled Release* **2001**, *71* (2), 183.

(41) Coniglio, A.; Stanley, H. E.; Klein, W. *Phys. Rev. Lett.* **1979**, *42* (8), 518.

(42) Meakin, P. *J. Colloid Interface Sci.* **1984**, *102* (2), 491.

(43) Witten, T. A.; Sander, L. M. *Phys. Rev. Lett.* **1981**, *47* (19), 1400.

(44) Miwa, K.; Deguchi, T. *J. Phys. Soc. Jpn.* **2003**, *72* (5), 976.

(45) Miwa, K.; Deguchi, T. *J. Phys. Soc. Jpn.* **2005**, *74* (2), 554.

(46) Ohno, K.; Kawazoe, Y. *Comput. Theor. Polym. Sci.* **2000**, *10* (3−4), 269.

(47) Manneville P. de Seze, L. In *Numerical methods in the study of critical phenomena*; Della Dora, I., Demangeot, J., Lacolle, B., Eds.; Springer-Verlag: Berlin, 1981; p 116.

(48) Bansil, R.; Herrmann, H. J.; Stauffer, D. *Macromolecules* **1984**, *17* (5), 998.

(49) Ghiass, M.; Rey, A. D.; Dabir, B. *Polymer* **2002**, *43* (3), 989.

(50) Herrmann, H. J.; Landau, D. P.; Stauffer, D. *Phys. Rev. Lett.* **1982**, *49* (6), 412.

(51) Bowman, C. N.; Peppas, N. A. *J. Polym. Sci., Part A: Polym. Chem.* **1991**, *29* (11), 1575.

(52) Bowman, C. N.; Peppas, N. A. *Chem. Eng. Sci.* **1992**, *47* (6), 1411.

(53) Ward, J. H.; Peppas, N. A. *Macromolecules* **2000**, *33* (14), 5137.

(54) Otsu, T.; Yoshida, M. *Makromol. Chem., Rapid Commun.* **1982**, *3* (2), 127.

(55) Ward, J. H.; Shahar, A.; Peppas, N. A. *Polymer* **2002**, *43* (6), 1745.

(56) Hutchison, J. B.; Anseth, K. S. *Macromol. Theory Simul.* **2001**, *10* (6), 600.

(57) Ping, G.; Yuan, J. M.; Vallieres, M.; Dong, H.; Sun, Z.; Wei, Y.; Li, F. Y.; Lin, S. H. *J. Chem. Phys.* **2003**, *118* (17), 8042.

(58) Levi L. Srebnik, S. *Macromol. Symp.* . in press.

(59) Metropolis, N.; Rosenbluth, A. W.; Rosenbluth, M. N.; Teller, A. H.; Teller, E. *J. Chem. Phys.* **1953**, *21* (6), 1087.

(60) Panyukov, S.; Rabin, Y. *Macromolecules* **1996**, *29* (26), 8530.

(61) Goodner, M. D.; Lee, H. R.; Bowman, C. N. *Ind. Eng. Chem. Res.* **1997**, *36* (4), 1247.

(62) Wen, M.; Scriven, L. E.; McCormick, A. V. *Macromolecules* **2003**, *36* (11), 4140.

(63) Wen, M.; Scriven, L. E.; McCormick, A. V. *Macromolecules* **2003**, *36* (11), 4151.

(64) Diamond, K. L.; Pandey, R. B.; Thames, S. F. *J. Chem. Phys.* **2004**, *120* (24), 11905.

(65) Ward, J. H.; Peppas, N. A. *Macromolecules* **2000**, *33*, 5137.

(66) Burdick, J. A.; Lovestead, T. M.; Anseth, K. S. *Biomacromolecules* **2003**, *4* (1), 149.

(67) Yavuz, H.; Karakoc, V.; Turkmen, D.; Say, R.; Denizli, A. *Int. J. Biol. Macromol.* **2007**, *41* (1), 8.

(68) Enoki, T.; Tanaka, K.; Watanabe, T.; Oya, T.; Sakiyama, T.; Takeoka, Y.; Ito, K.; Wang, G. Q.; Annaka, M.; Hara, K.; Du, R.; Chuang, J.; Wasserman, K.; Grosberg, A. Y.; Masamune, S.; Tanaka, T. *Phys. Rev. Lett.* **2000**, *85* (23), 5000.

(69) Atta, A. M.; Arndt, K. F. *J. Appl. Polym. Sci.* **2005**, *97* (1), 80.

(70) Alvarez-Lorenzo, C.; Guney, O.; Oya, T.; Sakai, Y.; Kobayashi, M.; Enoki, T.; Takeoka, Y.; Ishibashi, T.; Kuroda, K.; Tanaka, K.; Wang, G. Q.; Grosberg, A. Y.; Masamune, S.; Tanaka, T. *Macromolecules* **2000**, *33* (23), 8693.

(71) Spivak, D. A. *Adv. Drug Delivery Rev.* **2005**, *57* (12), 1779.

JP9087767